School of Medicine Publications and Presentations

School of Medicine

4-1-2022

Patients with chronic pain exhibit individually unique cortical signatures of pain encoding

Astrid Mayr

Pauline Jahn

Anne Stankewitz

Bettina Deak

Anderson M. Winkler

See next page for additional authors

Authors

Astrid Mayr, Pauline Jahn, Anne Stankewitz, Bettina Deak, Anderson M. Winkler, Viktor Witkovsky, Ozan Eren, Andreas Straube, and Enrico Schulz

RESEARCH ARTICLE

Patients with chronic pain exhibit individually unique cortical signatures of pain encoding

Astrid Mayr[1,2] | Pauline Jahn[2] | Anne Stankewitz[2] | Bettina Deak[2] |
Anderson Winkler[3] | Viktor Witkovsky[4] | Ozan Eren[2] | Andreas Straube[2] |
Enrico Schulz[2,5]

[1]Department of Radiology, University Hospital LMU, Ludwig-Maximilians-Universität München, Munich, Germany

[2]Department of Neurology, University Hospital LMU, Ludwig-Maximilians-Universität München, Munich, Germany

[3]Emotion and Development Branch, National Institute of Mental Health, National Institutes of Health, Bethesda, Maryland, USA

[4]Department of Theoretical Methods, Institute of Measurement Science, Slovak Academy of Sciences, Bratislava, Slovak Republic

[5]Department of Medical Psychology, Ludwig-Maximilians-Universität München, Munich, Germany

Correspondence
Astrid Mayr, Klinikum der Universität München, Klinik und Poliklinik für Neurologie, A: Fraunhoferstr. 20, 82152 Martinsried, Germany.
Email: am@pain.sc

Funding information
Deutsche Forschungsgemeinschaft, Grant/Award Number: SCHU2879/4-1

Abstract
Chronic pain is characterised by an ongoing and fluctuating intensity over time. Here, we investigated how the trajectory of the patients' endogenous pain is encoded in the brain. In repeated functional MRI (fMRI) sessions, 20 patients with chronic back pain and 20 patients with chronic migraine were asked to continuously rate the intensity of their endogenous pain. Linear mixed effects models were used to disentangle cortical processes related to pain intensity and to pain intensity changes. At group level, we found that the intensity of pain in patients with chronic back pain is encoded in the anterior insular cortex, the frontal operculum, and the pons; the change of pain in chronic back pain and chronic migraine patients is mainly encoded in the anterior insular cortex. At the individual level, we identified a more complex picture where each patient exhibited their own signature of endogenous pain encoding. The diversity of the individual cortical signatures of chronic pain encoding results bridge between clinical observations and neuroimaging; they add to the understanding of chronic pain as a complex and multifaceted disease.

KEYWORDS
BOLD, chronic pain, endogenous pain, fMRI, insular cortex

1 | INTRODUCTION

The perception of pain is a subjective and multidimensional experience that has a profound impact on the physiological and psychological state of an individual (Baliki et al., 2006; Moriarty, McGuire, & Finn, 2011). Chronic pain states are characterised by a hypersensitisation of nociceptive neurons (Gold & Gebhart, 2010), a reduced endogenous inhibition of the nociceptive system (Edwards, 2005; Henderson et al., 2013; Staud, 2012), and by maladaptive cortical processes (Phillips, 2009; Price, 2000). The neural mechanisms that underlie the process of

chronification are poorly understood. Previous studies found the amygdala, the medial prefrontal cortex, and the nucleus accumbens to be important in the transition from subacute to chronic back pain (CBP; Hashmi et al., 2013; Makary et al., 2020); the activity of the posterior hypothalamus is suggested to differentiate between patients with episodic and chronic migraine (CM; Schulte, Allers, & May, 2017).

The cortical regions that are involved in the processing of chronic pain have primarily been investigated with experimentally applied exogenous pain, that is, thermal (Baliki, Geha, Fields, & Apkarian, 2010; Gollub et al., 2018; Schwedt, Krauss, Frey, & Gereau, 2011; Vachon-Presseau et al., 2016), electrical (Callan, Mills, Nott, England, & England, 2014; Diers et al., 2007; Lloyd, Findlay, Roberts, & Nurmikko, 2008),

Astrid Mayr and Pauline Jahn contributed equally to this work.

mechanical (Giesecke et al., 2004; Gracely, Petzke, Wolf, & Clauw, 2002; Grossi et al., 2011; Kobayashi et al., 2009), or chemical stimulation (Schulte et al., 2017; Stankewitz, Aderjan, Eippert, & May, 2011). These studies found increased activity in patients with chronic pain in regions already known to be involved in the encoding of acute pain, such as the primary and secondary somatosensory cortices (S1, S2), sections of the insular and cingulate cortices, the cerebellum, and the thalamus (Apkarian, Bushnell, Treede, & Zubieta, 2005; Baliki et al., 2006; Filippi & Messina, 2020; Malinen et al., 2010; Price, 2000). However, applying experimental pain to patients and investigating pain-unspecific cortical networks may reveal cortical processes that are not necessarily at the core of the pain disease.

What matters to the individual, however, are the dynamics of *their* endogenous pain experience, which fluctuates over time and consists of periods of increasing, stable, and decreasing pain intensity. A number of studies have utilised this experimental approach with CBP patients continuously evaluating their spontaneously fluctuating pain without external stimulation (Baliki et al., 2006; Hashmi, Baliki, et al., 2012; Hashmi, Baria, et al., 2012; May et al., 2019). Imaging studies have reported higher activity in the medial prefrontal cortex for high pain compared to low pain intensity. Similarly, larger amplitudes of neuronal gamma oscillations have been recorded for higher pain intensities at frontocentral electrode sites in EEG (May et al., 2019). When contrasting periods of increasing pain to periods of stable and decreasing pain, Baliki and colleagues found an effect in the right anterior and posterior insula, S1 and S2, the middle cingulate cortex, and the cerebellum (Baliki et al., 2006). However, the investigation of pain intensity coding should not be restricted to periods of increasing pain (Baliki, Baria, & Apkarian, 2011; May et al., 2019), but also be assessed during periods of decreasing pain. Additionally, in some patients, lower intensities of pain have been assessed only during the second half of the experiment and higher pain intensities in the second half, which renders it impossible to exclude the effect of the order (May et al., 2019). As a methodological challenge in continuous and event-free imaging studies, it is important to preserve the naturally evolving cortical trajectory of the patients' endogenous pain. For the present study, using functional MRI (fMRI), we took a number of measures to tackle these issues, for example, (a) preserving the natural autocorrelation of the pain time courses, (b) applying only moderate data filtering, and (c) excluding recordings with pain time courses that do not exhibit any fluctuation.

Here, we aimed to assess the neuronal underpinnings of the natural fluctuations of spontaneous pain in four repeated sessions of functional imaging of two chronic pain diseases: CBP and CM. Both groups were chosen in order to investigate pain diseases with distinct aetiology and potentially distinct cortical processing. Extended and continuous recordings in repeated sessions enable us to capture balanced periods of rising, stable, and falling pain in all participants. The experimental design allows us to disentangle the cortical underpinnings of pain intensity encoding from the cortical mechanisms of intensity change detection (increasing, decreasing pain), as well as from cortical mechanisms of decision-making, motor processing and changes of visual input.

We hypothesise that the processing of endogenous pain yields a variety of individual patterns of cortical activity with a large amount of commonly activated brain regions in each patient group. We expect gradual changes of these common regions between patients and some individually specific activities in other regions. We expect to observe more similarity within a group than between both pain groups.

2 | MATERIALS AND METHODS

2.1 | Participants

The study included 20 patients diagnosed with CBP (−16 females; aged 44 ± 13 years) and 20 patients with CM (18 females; aged 34 ± 13 years). All participants gave written informed consent. The study was approved by the Ethics Committee of the Medical Department of the Ludwig-Maximilians-Universität München and conducted in conformity with the Declaration of Helsinki.

CBP patients are diagnosed according to the IASP criteria (The International Association for the Study of Pain; Merskey & Bogduk, 1994), which includes a disease duration of more than 6 months (mean CBP: 10 ± 7 years). All patients were seen in a specialised pain unit. CM patients were diagnosed according to the ICHD-3 (Headache Classification Committee of the International Headache Society (IHS), 2018), defined as a headache occurring on 15 or more days/month for more than 3 months, which, on at least 8 days/month, has the features of migraine headache (mean CM: 15 ± 12 years). All CM patients were seen in a tertiary headache centre.

All patients were permitted to continue their pharmacological treatment at a stable dose (Supplementary Tables 1 and 2). The patients did not report any other neurological or psychiatric disorders, or had contraindications for an MRI examination. Patients who had any additional pain were excluded (e.g., patients with migraine and back pain). For all patients, pain was fluctuating and not constant at the same intensity level. Patients with no pain or during headache attacks on the day of the measurement were asked to return on a different day. Patients were characterised using the German Pain Questionnaire (Deutscher Schmerzfragebogen; Casser et al., 2012) and the German version of the Pain Catastrophizing Scale (PCS; (Sullivan, Bishop, & Pivik, 1995); Supplementary Tables 1 and 2). The pain intensity describes the average pain in the last 4 weeks from 0 to 10 with 0 representing no pain and 10 indicating maximum imaginable pain (please note that this scale differs from the one used in the fMRI experiment). The German version of the Depression, Anxiety and Stress Scale was used to rate depressive, anxiety, and stress symptoms over the past week (Lovibond & Lovibond, 1995).

Patients were compensated with 60€ per session. In total nine screened patients were excluded: two patients developed additional pain during the study, the pain ratings of five patients were constantly increasing or decreasing throughout the pain rating experiment, and two patients were unable to comply with study requests. Then, 36 patients were recorded four times across 6 weeks with a gap of at least 2 days (CBP = 9 ± 12 days, CM = 12 ± 19 days) between

sessions. Four patients (2 CBP and 2 CM) were recorded three times. Due to the required data filtering, a steadily increasing time course of pain ratings is not suitable for fMRI analyses. The exclusion is an important prerequisite for the statistical independence of the three entities that describe the processing of chronic pain (see below).

2.2 | Experimental procedure

During the recording of fMRI, patients rated the intensity of their ongoing pain for 25 min using an MRI-compatible potentiometer slider (Schulz, Stankewitz, Witkovský, Winkler, & Tracey, 2019). The scale ranged from 0 to 100 in steps of five with 0 representing no pain and 100 representing the highest experienced pain. On a light grey screen a moving red cursor on a dark grey bar (visual analogue scale [VAS]) and a number above (numeric analogue scale [NAS]) were shown during the entire fMRI session. The screen was visible through a mirror mounted on top of the MRI head coil. Patients were asked to look only at the screen, focus on their pain with an emphasis on rising and falling pain. The intensity and the changes of perceived pain had to be indicated as quickly and accurately as possible. Each patient had sufficient practice outside the scanner to get familiarised with the rating procedure. To minimise head movement, foams were placed around the head and patients were told to lie as still as possible.

To control for visual-motor performance and decision-making activity during the pain rating session, a visual control experiment was carried out during the last visit. Patients were asked to continuously rate the changing background brightness of the screen as accurately and quickly as possible. The same feedback in the form of a red bar (VAS) and a number (NAS) was given on the same screen as for the pain-rating experiment. Unbeknownst to the patient, the control condition was a composition of parts of the previous pain rating sessions to match with range and frequency of the pain rating. Pain ratings between 0 and 100 in steps of 5 were converted to 21 shades of grey, 0 indicating black ([RGB: 0 0 0]) and 100 indicating white ([RGB: 255 255 255]).

2.3 | Data acquisition

Data were recorded on a clinical 3 T MRI scanner (Siemens Magnetom Skyra, Germany) using a 64-channel head coil. A T2*-weighted BOLD (blood oxygenation level dependent) gradient echo sequence with echo-planar image acquisition and a multiband factor of 2 was used with the following parameters: number of slices = 46; repetition time/echo time = 1,550/30 ms; flip angle = 71°; slice thickness = 3 mm; voxel size = 3 × 3 × 3 mm^3; field of view = 210 mm. Then, 1,000 volumes were recorded in 1,550 s. Field maps were acquired in each session to control for B0-effects. For each patient, T1-and T2-weighted anatomical MRI images were acquired using the following parameters for T1: repetition time/echo time = 2,060/2.17 ms; flip angle = 12°; number of slices = 256; slice thickness = 0.75 mm; field of view = 240 mm, and for T2: repetition time/echo time = 3,200/560 ms; flip angle = 120°; number of slices = 256; slice thickness = 0.75 mm; field of view = 240 mm.

2.4 | Data processing—Behavioural data

The rating data were continuously recorded with a variable sampling rate but downsampled offline at 10 Hz. To remove the same filtering effects from the behavioural data as from the imaging data, we applied a 400 s high-pass filter (see below). The rating data were convolved with a hemodynamic response function (HRF) implemented in SPM12 (Penny, Friston, Ashburner, Kiebel, & Nichols, 2011) with the following parameters: HRF = spm_hrf(0.1,[6 16 1 1,100 0 32]). The poststimulus undershoot was minimised by the ratio of response to undershoot and motivated by the continuous and event-free fMRI design. For the statistical analysis, the resulting filtered time course was transferred to MATLAB (MathWorks; version R2018a) and downsampled to the sampling frequency of the imaging data (1/1.55 Hz).

To allow for some variability in the HRF responses between pathological populations (two different conditions), as well as between different tasks (encoding of pain intensity changes and encoding of motor activity), systematic shifting of the rating vector and BOLD response between −15 and 20 s in steps of 1 s (36 steps) was applied (see explanations for Supplementary Figures 5 and 6). To disentangle the distinct aspects of pain intensity (AMP—amplitude) from cortical processes related to the sensing of rising and falling pain, we computed the ongoing rate of change (SLP—slope, encoded as 1, −1, and 0) in the pain ratings. The rate of change is calculated as the slope of the regression of the least squares line across a 3 s time window of the 10 Hz pain rating data. Periods coded as 0 indicate time frames of constant pain. We applied the same shifting (36 steps) as for the amplitude time course. The absolute slope of pain ratings (aSLP—absolute slope, encoded as 0 and 1), represents periods of motor activity (slider movement), changes of visual input (each slider movement changes the screen), and decision-making (each slider movement prerequisites a decision to move). Periods coded as 0 indicate time frames of constant pain without the need to move the slider. We deliberately kept the SLP and aSLP as nominal variables; a higher velocity of slider movement or a faster change of pain intensity are unlikely to cause a proportional change in brain activity. The low correlations of the three entities (AMP, SLP, aSLP) indicate the independence of the vectors. The mean (±SD) correlation coefficients (Fisher-z transformed) for all patients (CBP/CM) for each of the variable pairs were: r(AMP, SLP) = .007(±0.04)/.02(±0.04); r(SLP, aSLP) = .06(±0.2)/.01(±0.12); r(AMP, aSLP) = .002(±0.08)/−.004 (±0.09). The rating time courses were required to fluctuate at a relatively constant level, in order to mitigate potential effects of order (e.g., in case of continuously rising pain). To ensure the behavioural task performance of the patients fulfilled this criterion, the ratings of each patient's pain was evaluated based on a constructed parameter PR (see explanations after Supplementary Figure 1a,b).

2.5 | Data processing—Imaging data

fMRI data were preprocessed using FSL (version 5.0.10; Jenkinson, Beckmann, Behrens, Woolrich, & Smith, 2012), which included removal

of non-brain data (using brain extraction), slice time correction, head motion correction, B0 unwarping, spatial smoothing using a Gaussian kernel of full width at half maximum 6 mm, a nonlinear high-pass temporal filtering with a cutoff of 400 s, and spatial registration to the Montreal Neurological Institute template. The data were further semi-automatically cleaned of artefacts with MELODIC (Salimi-Khorshidi et al., 2014). Artefact-related components were evaluated according to their spatial or temporal characteristics and were removed from the data following the recommendations in Griffanti et al. (2014) and Kelly et al. (2010). The average number of artefact components for CM was 40 ± 6 and for CBP 49 ± 8. None of the recordings needed to be discarded due to excessive movement (>2 mm or 2° in any direction, see Supplement). We deliberately did not include any correction for auto-correlation, neither for the processing of the imaging data nor for the processing of the pain rating time course as this step has the potential to destroy the natural evolution of the processes we aim to investigate (see PALM analysis below).

2.6 | Statistical analysis—Imaging data

Using linear mixed effects (LME) models (MixedModels.jl package in Julia; (Bezanson, Edelman, Karpinski, & Shah, 2015), we aimed to determine the relationship between fluctuating pain intensity and the fluctuating cortical activity separately for each voxel. The fluctuating BOLD activity of a particular brain voxel is modelled through the time course of the three variables (AMP, SLP, aSLP) derived from the pain ratings (Figure 1).

In the description below, the statistical model is expressed in Wilkinson notation; the included fixed effects (fmri ∼ AMP + SLP + aSLP) describe the magnitudes of the population common intercept and the population common slopes for the relationship between cortical data and the intercept and these three variables. The added random effects (e.g., AMP − 1 | session) model the specific intercept differences for each recording session (e.g., session specific differences in pain levels or echo-planar image signal intensities):

$$\text{fmri} \sim \text{AMP} + \text{SLP} + \text{aSLP} + (\text{AMP} - 1 | \text{session}) + (\text{SLP} - 1 | \text{session}) + (\text{aSLP} - 1 | \text{session}) \quad (1)$$

AMP
50
30
10

change - SLP
motor - aSLP
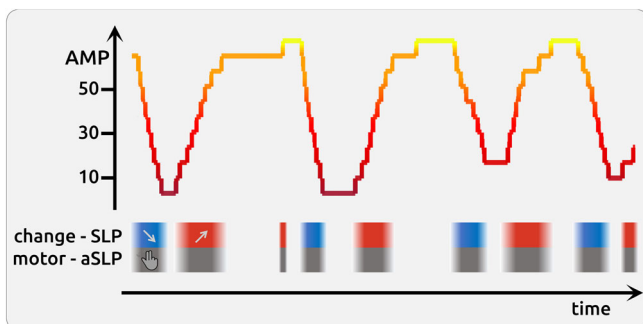
time

FIGURE 1 Schematic illustration of a 5 min fluctuating time course of pain rating

The common slope and the common intercept represent the group-wise fixed effects, which are the parameters of main interest in the LME. Hence, the model has four fixed effects parameters (common intercept, AMP, SLP, aSLP) and 234 (3 × 78) random effect parameters with related variance components of AMP random slopes, SLP random slope, aSLP random slope, and additive unexplained error. Each model was computed 36 times along the time shifts of the rating vector (−15 to 20 s in steps of 1 s, Supplementary Material on shifting). This procedure results in 36 t-values for each modality (AMP, SLP, and aSLP) and voxel. For each modality, the highest absolute t-values of the fixed effect parameters between −15 and 20 s were extracted.

Although the group statistics was not the main focus of the study, and despite the large variance of the findings across patients, we computed a direct comparison between the pain rating task and the visual control task:

$$\text{fmri} \sim \text{AMP} \times \text{condition} + \text{SLP} \times \text{condition} + \text{aSLP} \times \text{condition} + (0 + \text{AMP} | \text{session}) + (0 + \text{SLP} | \text{session}) + (0 + \text{aSLP} | \text{session}) \quad (2)$$

For completeness, we also computed the comparison between CBP and CM:

$$\text{fmri} \sim \text{AMP} \times \text{CBPvsCM} + \text{SLP} \times \text{CBPvsCM} + \text{aSLP} \times \text{CBPvsCM} + (0 + \text{AMP} | \text{session}) + (0 + \text{SLP} | \text{session}) + (0 + \text{aSLP} | \text{session}) \quad (3)$$

The model equation reflects how each fixed effect is differently modulated by condition (pain vs. visual). We included all four pain rating sessions into the analysis.

The statistical model also included the information of the direction of change of pain intensity (SLP: encoded as −1 as shown in blue boxes for negative slope; encoded as 0 for stable phases of pain, and encoded as 1 as shown in red boxes for increasing pain). The task also required moving the potentiometer slider (aSLP: encoded as 1 as shown in grey for motor phases, and encoded as 0 for stable phases that did not require a motor process). Brain estimates of amplitude (AMP) should be independent irrespective of whether a data point originates from rising, stable or falling time points of the rating time course. In a similar vein, each slider movement involves a prior decision-making and motor activity. These processes (SLP, aSLP) occur concomitant to the encoding of pain intensity (AMP) but are functionally, temporally and statistically independent.

2.7 | Correcting statistical testing—Surrogate data

All voxel-wise statistical tests had to be corrected for multiple testing (voxels, time shifts) and autocorrelation in the behavioural data: we created 1,000 surrogate time courses using the iterative amplitude adjusted Fourier transform algorithm from the original rating data, which were uncorrelated to the original rating data but had the same autocorrelation structure as the original data (Schreiber & Schmitz, 1996). Using surrogate data, the entire LME analysis was

repeated 1,000 times for the vectors (AMP, SLP, aSLP) with zero shift, resulting in 1,000 whole-brain statistical maps for AMP, SLP, and aSLP, respectively. From each map the highest absolute t-values of each repetition across the whole volume was extracted. This procedure resulted in a right-skewed distribution of 1,000 values for each condition. Based on the distributions of 1,000 values (for AMP, SLP, aSLP), the statistical thresholds were determined using the "palm_datapval.m" function publicly available in PALM (Winkler et al., 2016; Winkler, Ridgway, Webster, Smith, & Nichols, 2014).

2.8 | Comparisons of topographies

We tested whether the topography of the amplitude encoding (AMP) resembles the topography of the neurological signature of applied physical pain (Neurologic Pain Signature [NPS]; Wager et al., 2013). We thresholded the NPS weights map at 0.005 and the AMP map at $t > 2$ and "normalised" both maps with the following procedure: the preselected absolute values were ranked and equidistant numbers between 1 and 1,000 were given to each included voxel. Voxels with negative t-values were given back their negative sign. Spatial correlations using Kendall's τ (tau) coefficients were computed for the common superthreshold voxels (4,900 voxels for CM; 1,966 voxels for CBP) of the NPS map and the group activity map.

We also investigated the individual maps of endogenous pain encoding separately for each participant across all recordings. To assess whether the pattern of activity resembles the map of the group statistics, we correlated the activity of the group maps with the activity of the single-patient maps. The data were restricted to the voxels of group statistics and single-subject statistics with an absolute t-value larger than 2. We "normalised" group map and single-patient maps with the following procedure: the preselected absolute t-values were ranked and equidistant numbers between 1 and 1,000 were given to each included voxel. Voxels with negative t-values were given back their negative sign. Separately for each patient, spatial correlations using Kendall's τ (tau) coefficients were computed for each patient's activity map with the group activity map for the common superthreshold voxels.

3 | RESULTS

3.1 | Questionnaires

The mean pain intensity specified in the questionnaires was $5 \pm 2/10$ for CBP and $5 \pm 1/10$ for CM. The mean duration of the chronic pain was 10 ± 7 years for CBP and 15 ± 12 years for CM. The scores for the PCS were $17 \pm 10/52$ for CBP and $21 \pm 10/52$ for CM. For CBP, the depression scale was $4 \pm 3/21$, the anxiety scale $3 \pm 2/21$, and the stress scale $7 \pm 4/21$. For CM, the depression scale was $3 \pm 3/21$, the anxiety scale $3 \pm 4/21$, and the stress scale $6 \pm 4/21$ (mean $\pm$ SD/maximum). Both groups did not differ from each other regarding behavioural variables, age, and disease duration (two-sample t tests,

$p > .05$). Supplementary Tables 1 and 2 contain detailed patient characteristics, questionnaire data, and cutoffs.

3.2 | Behavioural data

The average pain ratings were variable between recording sessions (see Supplementary Figures 2 and 3 for the detailed rating time courses of each session). For CBP and CM, we found an average rating of 39 ($\pm$14) and 40 ($\pm$15), respectively. The pain ratings within each session were fluctuating substantially, as reflected by a high variance over the 25 min of recording: $\sigma^2 = 109.3$ ($\pm$126.6) for CBP and $\sigma^2 = 93.3$ ($\pm$62.8) for CM. Due to the prerequisites of a low PR score, the average rating did not exhibit any systematic change over the time course of one experimental session. In general, we found a minimal positive slope of 0.13 ($\pm$0.41; mean change of rating unit per minute) for CBP and of -0.05 ($\pm$0.37) for CM (all mean $\pm$ SD).

3.3 | Imaging results

Voxel-wise LMEs were computed to identify the brain regions in which the cortical activity changed during the experiment with respect to the amplitude of the pain rating (amplitude—AMP), as well as to rising or falling pain (slope—SLP). Each change of pain rating, irrespective of direction, is accompanied by motor activity, decision-making processes, and the perception of visual change on the monitor (aSLP). Respective time courses of AMP, SLP, and aSLP were related to the time courses of brain activity in order to obtain a statistical estimate of the cortical underpinnings of these independent processes. T-values of the fixed-effects parameters quantify the relationships. The model was separately calculated for CM and CBP.

3.4 | Encoding of pain intensity across all CBP patients (AMP)

We found the subjective intensity of endogenous pain is encoded in the anterior insular cortex (AIC), the frontal operculum, and the pons. We also found regions that exhibit decreased activity with higher pain intensities: the posterior cingulate cortex (PCC), the precuneus, the pregenual anterior cingulate cortex (pACC), and the hippocampus (Figure 2a; Supplementary Figure 7; Table 1). These findings persist when computing the contrast (Equation (3) between the pain and the visual condition. We found a spatial correlation between AMP and the NPS map of 0.31 ($p < .001$).

3.5 | Encoding of the change of pain intensity across all CBP patients (SLP)

The cortical processes that reflect the change of pain intensity are located in the AIC, in various regions in the frontal lobe (frontal orbital

cortex, frontal operculum, middle frontal gyrus), as well as in the pACC, PCC, and parahippocampal gyrus. Brain regions that exhibit decreased activity during increasing pain comprise regions in the occipital lobe (occipital pole, lateral occipital cortex), the precuneus, the pACC, and PCC, the paracingulate gyrus and the brainstem (Figure 2b; Supplementary Figure 8; Table 2). The direct comparison between the pain condition and the visual control condition confirms the findings for the bilateral AIC and for the frontal lobe.

3.6 | Processing of motor activity and decision-making across all CBP patients (aSLP)

For the processing of motor activity, decision-making, and changes of visual input, we found increased activity in the parietal lobe (superior parietal lobe, supramarginal gyrus), but also in the precentral and postcentral gyrus (M1/S1), the middle frontal gyrus, the cerebellum, the thalamus, and the PCC. Decreased activity was located mainly in the hippocampus, the parahippocampal gyrus, the superior temporal gyrus, the lateral occipital gyrus, and the precuneus (Figure 2c). To separate the largely overlapping clusters and to disentangle the contribution of the brain regions, we increased the threshold beyond the threshold of the randomisation statistics (Supplementary Table 3).

3.7 | Encoding of pain intensity across all CM patients (AMP)

For CM, mainly the cerebellum is positively related to the intensity of endogenous pain, as well as the frontal orbital cortex and the temporal fusiform cortex. We found areas that are negatively related to pain intensity in the PCC, the pACC and the subcallosal cortex, but also in the amygdala, and the thalamus (Figure 3a; Supplementary Figure 9; Table 3). There was no difference for the direct comparison between the pain condition and the visual condition. We found a spatial correlation between AMP and the NPS map of -0.08 ($p < .001$).

3.8 | Encoding of the change of pain intensity across all CM patients (SLP)

The processes that contribute to the change of pain intensity only activate the cerebellum and the AIC. Brain regions that exhibit decreased activity during increasing pain comprise various regions in the occipital lobe (occipital pole, lateral occipital cortex), as well as the angular gyrus, the precuneus, and the superior frontal gyrus (Figure 3b; Supplementary Figure 10; Table 4). There was no difference for the direct comparison between the pain condition and the visual condition.
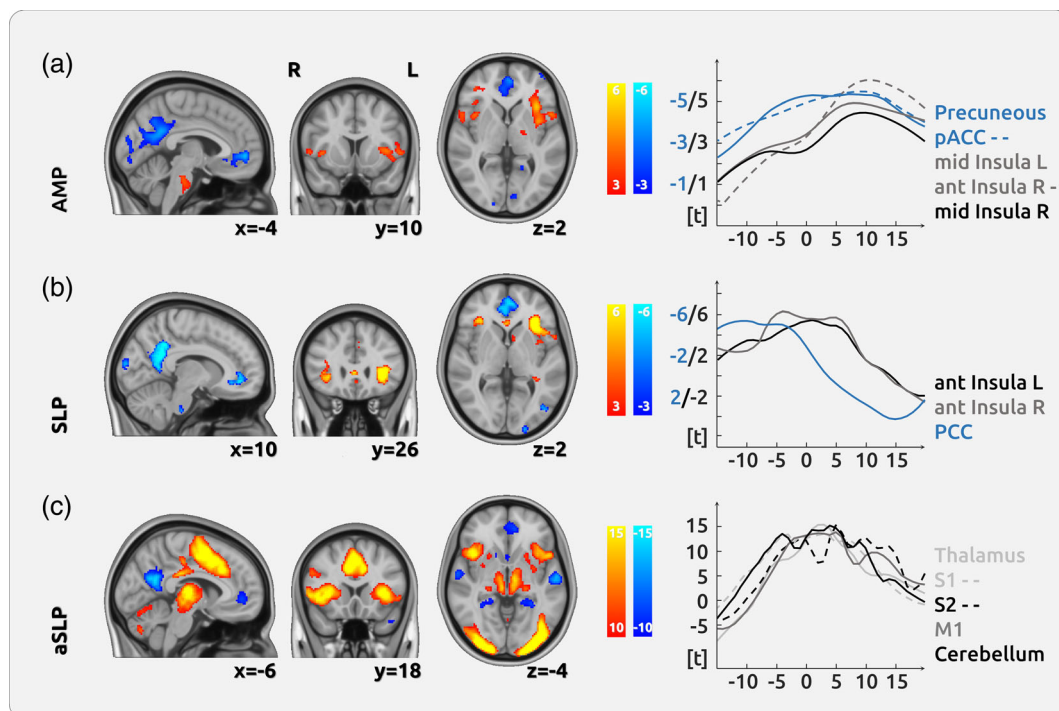
FIGURE 2 Cortical processing of chronic pain in chronic back pain (CBP). (a) The upper row shows the cortical encoding of the endogenous pain intensity (amplitude—AMP): the activities in the bilateral anterior insular cortex (AIC), the pons, and the frontal cortex were positively related to pain intensity. We found negative relationships between brain activity and pain intensity in the precuneus and the pregenual anterior cingulate cortex (pACC). (b) The processing of changes of pain intensity (slope—SLP) was mainly localised in the bilateral AIC. (c) The movement process, which prerequisites motor activity and decision-making (absolute slope—aSLP), shows a vast network of activity in the thalamus, the cingulate cortex, the entire insula and the cerebellum. The graphs on the right show the temporal dynamics of the haemodynamic delay for several regions in relation to the current pain rating (at time point 0 s)

TABLE 1 Active brain areas that encode pain intensity across all CBP patients

Anatomical structure	Cluster size	t-Value		Coordinates		
		pos	neg	x	y	z
Posterior cingulate cortex, precuneus cortex	3,712		−5.5	−1	−54	26
Anterior insular cortex, frontal operculum cortex	1862	5.78		−36	15	4
Occipital pole	906		−4.22	−2	−86	5
Anterior cingulate cortex, paracingulate gyrus	877		−5.23	0	43	−3
Lateral occipital cortex	434		−4.34	52	−61	27
Pons	403	4.23		−4	−21	−35
Frontal orbital cortex, frontal operculum cortex	327	4.23		38	25	0
Lateral occipital cortex	318		−4.02	−41	−64	30
Inferior frontal gyrus*	225	16.2		35	32	6
Hippocampus, parahippocampal gyrus	225		−4.59	27	−27	−15
Frontal pole	216	17.8		−33	52	24
Cerebellum (right VIIb)	170	3.95		31	−62	−49
Paracingulate gyrus*	141		−16.6	−2	53	−3
Superior frontal gyrus, middle frontal gyrus	117		−3.51	−27	19	58
Inferior frontal gyrus, precentral gyrus (M1)	115	3.97		55	10	4
Frontal pole*	113		−16.2	−39	59	−3
Frontal pole*	99		−20.2	36	62	−8
Anterior insular cortex	99	15		−31	16	7
Frontal pole	86		−3.58	−15	42	50
Middle temporal gyrus	69		−4.41	−60	−14	−11
Inferior frontal gyrus*	62	14.8		−33	31	4
Paracingulate gyrus*	56		−15	10	44	−4
Cerebellum (left IX)	51		−3.76	−9	−50	−41
Occipital fusiform gyrus, lingual gyrus	51		−3.75	24	−70	−6
Frontal pole	46		−3.93	−41	57	2
Subcallosal cortex	44		−4.02	0	6	−6
Superior frontal gyrus	43		−3.34	24	31	50
Cerebellum (right IX)	41		−3.01	6	−54	−35
Right pallidum	39	3.62		16	−3	7
Amygdala	33		−3.71	−11	−10	−14
Superior frontal gyrus, middle frontal gyrus	28		−3.51	−23	1	52
Frontal pole	24		−3.44	38	61	−5
Middle frontal gyrus	23		−3.4	−40	2	49
Frontal orbital cortex	18	3.62		−41	25	−21
Posterior cingulate cortex	17		−3.57	9	−38	11
Parahippocampal gyrus	16	3.22		−23	−32	−28
Middle frontal gyrus	13		−3.51	−51	25	25
Anterior cingulate cortex	11	3.62		0	20	18
Superior frontal gyrus	11		−3	−7	17	67
Superior temporal gyrus	11		−2.9	53	−9	−12

Abbreviation: CBP, chronic back pain.

3.9 | Processing of motor activity and decision-making across all CM patients (aSLP)

The processing of motor activity, decision-making, and changes of visual input shows a network of increased activity mainly in the insular cortex, the thalamus, the pallidum, the parietal lobe (superior parietal lobule, parietal operculum, supramarginal gyrus) and the cerebellum. Decreased activity was found in the precuneus, the hippocampus, the lateral occipital cortex, the superior frontal and superior temporal gyrus and the cerebellum (Figure 3c). To separate the large

TABLE 2 Active brain areas that encode the change of pain intensity across all CBP patients

Anatomical structure	Cluster size	t-Value		Coordinates		
		pos	neg	x	y	z
Frontal operculum cortex, anterior insular cortex	1738	7.74		−38	27	8
Precuneus cortex, posterior cingulate cortex	1,511		−6.86	4	−56	25
Paracingulate gyrus, anterior cingulate cortex	878		−6.43	0	44	−3
*Frontal operculum cortex, anterior insular cortex**	484	15.8		−33	23	5
Frontal orbital cortex, frontal operculum cortex, anterior insular cortex	259	5.74		35	28	2
Lateral occipital cortex	236		−5.78	49	−59	29
Occipital pole	232		−5.93	15	−94	14
Occipital pole	176		−5.84	−5	−90	18
Parahippocampal gyrus	173		−5.45	−24	−40	−10
Brain stem	163		−5.57	4	−26	−41
*Frontal orbital cortex**	154	14.6		35	28	−1
Lateral occipital cortex	144		−6.32	−45	−72	6
Parahippocampal gyrus	134	5.35		−30	−42	3
Anterior cingulate cortex	132	5.22		0	21	26
Subcallosal cortex	103		−6.16	0	8	−4
Hippocampus	96		−5.01	29	−23	−17
Occipital pole	92		−5.03	−20	−98	0
Left caudate	90	4.96		−7	4	7
Frontal pole	85		−5.69	23	40	44
Posterior cingulate cortex	83	4.64		−1	−26	22
Cerebellum (left IX)	82		−6.01	−8	−51	−47
Middle frontal gyrus	75	4.95		−36	34	35
Subcallosal cortex, anterior cingulate cortex	63	6.28		1	27	1
Occipital fusiform gyrus	61	4.96		28	−79	−20
Frontal pole	61	4.96		38	61	−7
Posterior cingulate cortex	43	4.87		−11	−39	16
Precentral gyrus (M1)	41	12.4		−55	6	4
Lingual gyrus	36		−5.02	−11	−70	−6
Precuneus cortex	33	4.84		−10	−72	48
Lingual gyrus, occipital pole	31		−4.63	−8	−90	−6
Occipital pole	28		−5.21	−28	−93	11
Middle temporal gyrus	26		−4.62	−60	−21	−7
Brain stem	26	4.45		−8	−20	−41
Cerebellum (left IX)	24	4.73		−10	−50	−38
Angular gyrus, superior parietal lobule	24	4.57		−38	−52	42
Paracingulate gyrus	21	3.55		17	36	−5
Supramarginal gyrus	18	4		−54	−42	31
Superior frontal gyrus	17		−4.17	24	23	61
Occipital pole	16	4.06		17	−94	−7
Precuneus cortex	16		−3.79	−18	−51	6
Temporal fusiform gyrus	14	3.95		−37	−35	−9
Anterior cingulate cortex	13	3.91		−13	34	−5
Cerebellum (right VIIb)	13	3.74		25	−73	−49
Brain stem	13	3.58		−15	−23	−13

(Continues)

TABLE 2 (Continued)

Anatomical structure	Cluster size	t-Value		Coordinates		
		pos	neg	x	y	z
Thalamus	13	3.46		18	−6	7
Temporal pole, middle temporal gyrus	13		−3.45	−48	2	−31
Brain stem	12	4.43		−11	−9	−35
Parietal operculum cortex	12		−3.67	−50	−25	15
Angular gyrus	11	3.81		−32	−58	23
Hippocampus	11	3.42		36	−33	−5

Abbreviation: CBP, chronic back pain.
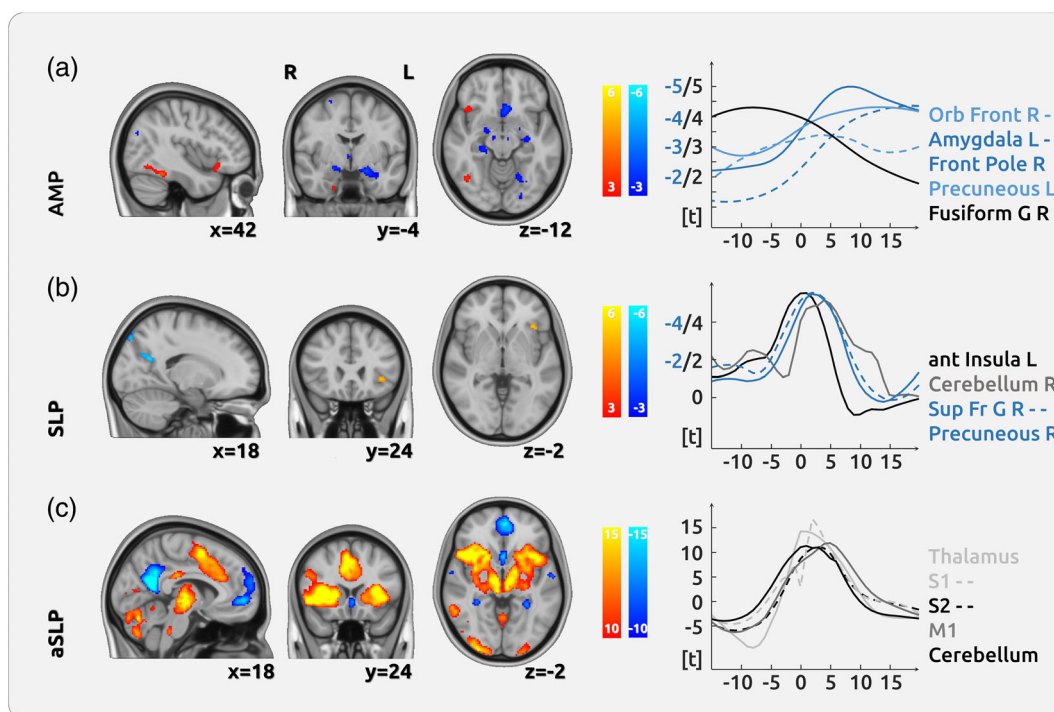
FIGURE 3 Cortical processing of chronic pain in chronic migraine (CM). (a) The upper row shows no major region that encodes the intensity of endogenous pain (amplitude—AMP). We found negative relationships between brain activity and pain intensity in the posterior cingulate cortex (PCC) and the pregenual anterior cingulate cortex (pACC). (b) The processing of changes of pain intensity (slope—SLP) was mainly localised in the left anterior insular cortex (AIC). Negative relationships were found in frontal and motor areas as well as in the precuneus. (c) The movement process, which prerequisites motor activity and decision-making (absolute slope—aSLP), shows a vast network of activity in the thalamus, the cingulate cortex, the entire insula, and the cerebellum. The graphs on the right show the temporal dynamics of the haemodynamic delay for several regions in relation to the current pain rating (at time point 0 s)

overlapping clusters and to disentangle the contribution of the brain regions, we increased the cluster threshold beyond the threshold of the randomisation statistics (Supplementary Table 4).

3.10 | Visual control experiment

In the control experiment, predominantly occipital areas (occipital pole, lateral occipital cortex and occipital fusiform gyrus) of the brain were activated for the CBP patient group only (*italic and with asterisk* * in Tables 1 and 2; Supplementary Table 5).

3.11 | Individual patterns of pain intensity encoding in single patients

We found a considerable variety of activation patterns for pain intensity encoding (AMP) across participants. Activation maps for AMP for all single patients are shown for CBP (Figure 4) and CM (Figure 5). While some patients exhibit a similar activity map to the maps from the group statistics, other patients show a weaker correlation with the activity pattern of the group statistics (Supplementary Figure 4a). This variability is also reflected by the substantial individual pain-related activity of AIC, as derived from

TABLE 3 Active brain areas that encode pain intensity across all CM patients

Anatomical structure	Cluster size	t-Value		Coordinates		
		pos	neg	x	y	z
Posterior cingulate cortex, precuneus cortex	4,995		−4.76	−4	−52	21
Anterior cingulate cortex	920		−4.03	−3	34	4
Amygdala	674		−3.99	−26	−5	−21
Amygdala, hippocampus	375		−3.7	21	−17	−12
Superior frontal gyrus	322		−3.19	25	−2	59
Subcallosal cortex	306		−3.8	−1	13	−7
Cerebellum (right VIIIa)	302	3.52		20	−65	−51
Occipital pole	279		−3.5	14	−94	17
Frontal pole	254		−3.79	−15	62	16
Frontal pole	226		−4.59	22	60	20
Frontal orbital cortex	175	3.77		47	20	−8
Thalamus	174		−4.2	13	−28	6
Temporal fusiform cortex	174	4.05		43	−51	−18
Middle temporal gyrus	171	3.42		53	−41	5
Cerebellum (right crus I)	103	3.37		49	−63	−42
Frontal pole	102		−3.51	34	59	3
Lateral occipital cortex	102		−3.34	42	−76	27
Cerebellum (left IX)	95	3.31		−8	−57	−51
Postcentral gyrus (S1), superior parietal lobule	62		−3.16	25	−40	73
Middle temporal gyrus	56	3.44		67	−43	−4
Precentral gyrus (M1)	49		−3.03	30	−21	69
Middle temporal gyrus	47		−3.44	−58	−55	1
Occipital pole	43		−3.5	−3	−98	17
Supramarginal gyrus	43		−3.3	36	−49	8
Precentral gyrus (M1)	41	3.4		61	6	7
Cerebellum (left VIIIa, VIIIb)	40	3.39		−27	−66	−55
Middle temporal gyrus	30	3.45		65	−20	−8
Parahippocampal gyrus	30	3.3		22	−5	−37
Temporal fusiform cortex	27	3.07		−28	−11	−39
Temporal fusiform cortex	25		−3.19	−38	−49	−2
Lateral occipital cortex	21		−3.08	22	−71	57
Intracalcarine cortex	19		−3.03	−6	−83	11
Lateral occipital cortex	18		−3.21	52	−65	20
Precuneus cortex	18		−2.98	−27	−54	11
Precentral gyrus (M1), posterior cingulate cortex	16		−2.94	−4	−30	48
Posterior insular cortex	14		−3.12	37	−8	5
Middle temporal gyrus	12	3.15		58	−19	−17
Occipital pole	11		−2.99	29	−93	13
Left caudate	11		−2.96	−16	−15	28

Abbreviation: CM, chronic migraine.

the peak of the group AMP statistics for CBP (Supplementary Figure 4b). The group and single-subject results of the shift distributions for CBP and CM are shown in Supplementary Figures 5 and 6 for AMP, SLP, and aSLP, respectively.

3.12 | Further analyses

In our view, the distinct individual patterns of pain-related cortical activity make any further analysis at group level obsolete; this applies

TABLE 4   Active brain areas that encode the change of pain intensity across all CM patients

Anatomical structure	Cluster size	t-Value pos	neg	Coordinates x	y	z
Lateral occipital cortex	187		−5.77	39	−77	32
Occipital pole	148		−5.89	−17	−97	−11
Lateral occipital cortex	116		−5.63	12	−80	48
Precuneus cortex	79		−6.09	17	−62	24
Superior frontal gyrus	71		−5.57	24	4	58
Cerebellum (right crus I)	38	5.19		39	−70	−30
Angular gyrus, middle temporal gyrus	28		−5.44	55	−55	14
Frontal orbital cortex, anterior insular cortex	25	5.28		−37	24	−2
Cerebellum (right crus I)	19	4.95		34	−78	−34

Abbreviation: CM, chronic migraine.

to the comparison between CBP and CM, as well as to an introduction of behavioural data. However, in order to provide a complete set of analyses, we directly compared the encoding of CBP and CM regarding AMP and SLP. For AMP, there are a few regions that are statistically different between CBP and CM. They show a stronger effect (positive or negative) for CBP (Supplementary Table 6). We did not find any difference for aSLP. Similar to the within group finding, the result of the between group comparison is likely based on the cortical processing of a subgroup of the CBP patients.

Given the individually distinct patterns for this study, we deliberately decided against including the behavioural variables into the statistical model. We would potentially find an effect, for example, of disease duration, in a small region of the brain. Because the individual maps exhibit enormous qualitative differences and distinct patterns, any potential correlation with behavioural variables would probably join the myriad of publications with unreliable results.

4 | DISCUSSION

Here, we aimed to investigate how the intensity and the intensity change of endogenous pain are subserved in the brain of patients with chronic pain. The experimental design resembles the everyday experience of these patients, which is characterised by naturally fluctuating pain and consists of phases of relatively low pain and phases of relatively high pain. Therefore, we are discussing the findings of the present study mainly in light of previous approaches to investigate endogenous and fluctuating chronic pain. Several novel methodological advances contribute to the current findings:

1. By making use of the event-free design, we took the entire time course of the data into account and related the trajectory of cortical processes to the fluctuating intensity of pain; we have identified brain regions that are involved in the encoding of pain intensity irrespective of whether the pain is currently rising, falling or stable. By using surrogate data as control, we were able keep the naturally evolving data structure intact.

2. We had a particular focus on a balanced time course of pain ratings, which allowed us to detect brain regions that encode transient states of increasing and decreasing pain; these processes could be targeted in a future neurofeedback study with the aim to facilitate decreasing pain.

3. Our statistical model included aspects that are not specific to pain processing and could disentangle these complementary and confounding aspects of the data, such as the aSLP variable, which comprises pain-unrelated decision-making, visual change processing, and motor activity. It must be noted that these three processes cannot be separated in the aSLP variable.

4. We emphasise the importance of a more patient-centred approach in neuroscience by repeatedly recording and analysing single patients. The continuous suffering from pain for many years revealed that each patient shows a unique pattern of cortical pain encoding, which can be considered as an individual signature of chronic pain processing. Many of the individual signatures only distantly resemble the result of the group statistics.

5. Our statistical approach with adjustable shifts between cortical processes and pain ratings allowed us to take into account the temporal dynamics of the continuous design. The variable shifts incorporate, on the one hand, individual variations of the HRF and, on the other hand, the individual cascade of cortical processes that precede and succeed the transient Intensity of pain.

4.1 | Encoding of pain intensity across all patients—AMP

For CBP patients, we found—across all patients and sessions—that the intensity of pain is mainly encoded in the AIC, the frontal operculum, and the pons. These regions exhibit a positive relationship between cortical activity and the amplitude of continuous pain ratings: higher intensities of pain are accompanied by higher cortical activity. Additionally, we found that higher intensities of endogenous pain in CBP are related to decreased activity in the PCC, pACC, the precuneus, the hippocampus, and several frontal and occipital regions. This
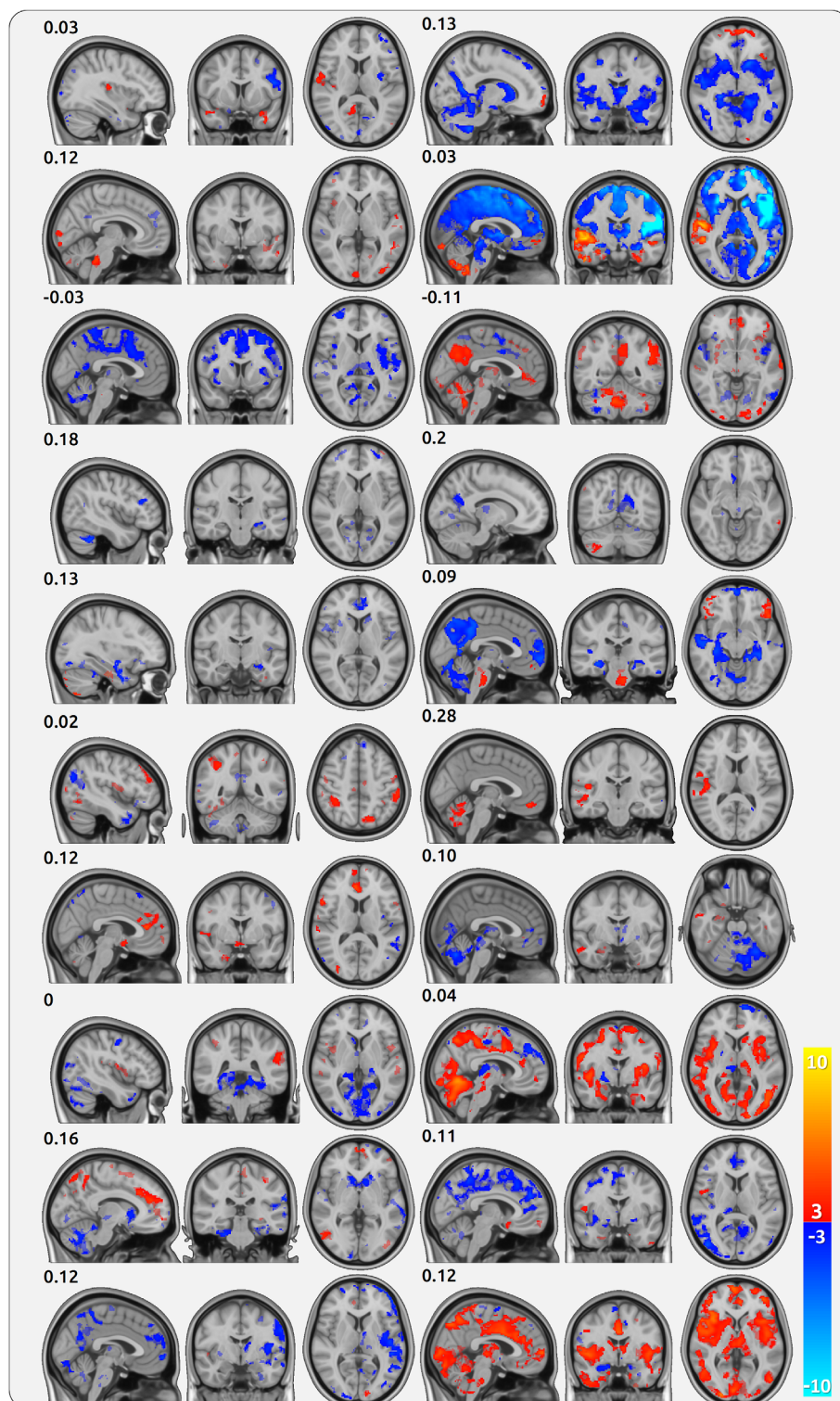
FIGURE 4 Cortical processing of single chronic back pain (CBP) patients. Each triplet of maps belongs to one patient (20 in total) and shows the cortical encoding of pain (AMP) across all sessions of the patient. The numbers indicate the spatial correlation of the individual map with the group map
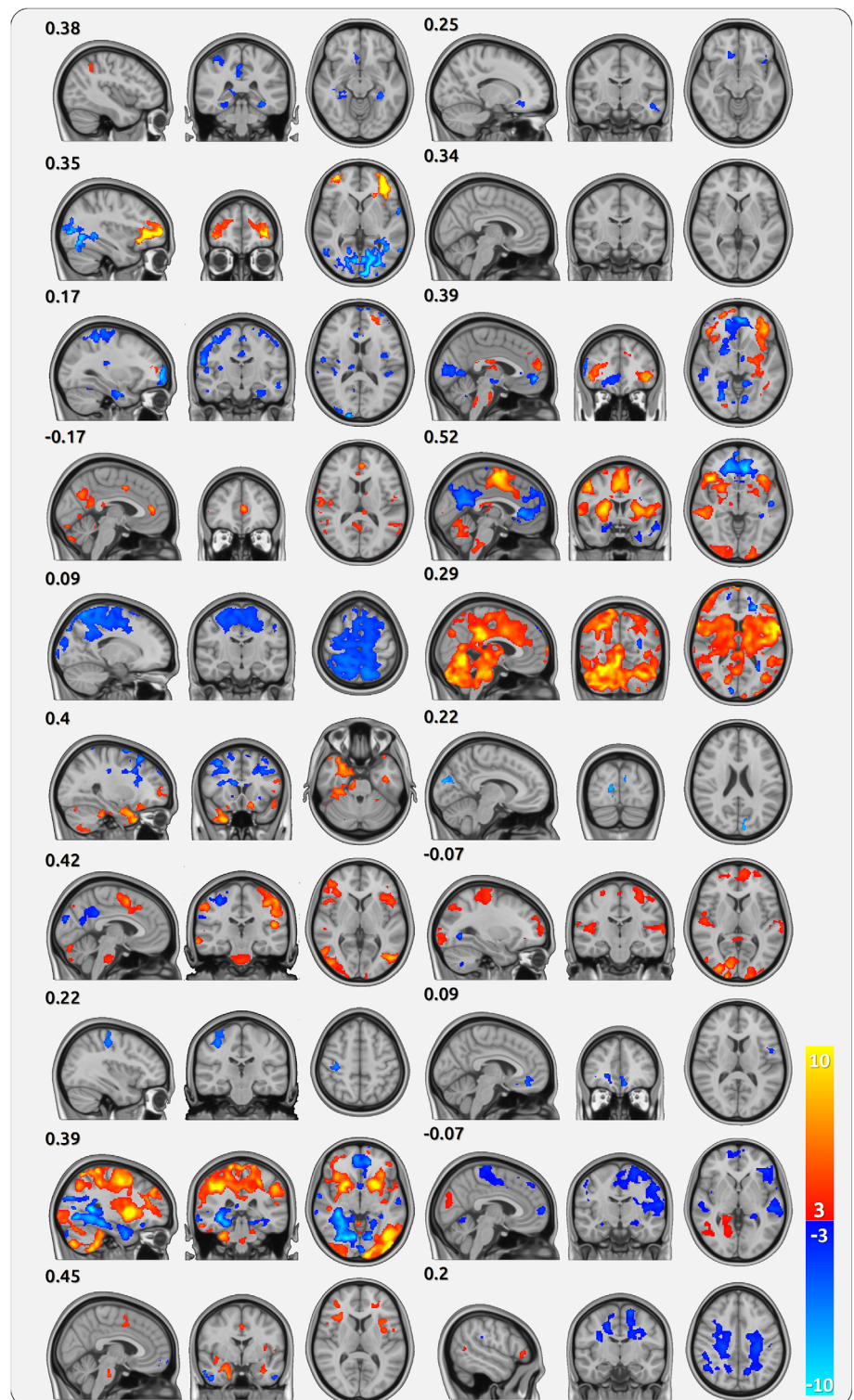
network of brain regions is largely overlapping with the NPS (Wager et al., 2013), but contradicts findings from previous work that located the encoding of endogenous chronic lower back pain predominantly in frontal regions (Baliki et al., 2006; Hashmi, Baliki, et al., 2012; Hashmi, Baria, et al., 2012).

For the encoding of the pain intensity in CM, we did not observe any cortical region within the NPS network but found a positive relationship between pain intensity and cortical activity predominantly in the cerebellum, as well as in the frontal orbital cortex and in the fusiform cortex. In addition, similar to the CBP patients, we found a negative relationship between pain intensity and brain activity in the PCC, pACC, and the precuneus, as well as in the amygdala and the subcallosal cortex. The absence of any single NPS region that codes for pain intensity in CM underlines the complex pathophysiology of

FIGURE 5 Cortical processing of single chronic migraine (CM) patients. Each triplet of maps belongs to one patient (20 in total) and shows the cortical encoding of pain (AMP) across all sessions of the patient. The numbers indicate the spatial correlation of the individual map with the group map

the disease (Burstein, Noseda, & Borsook, 2015; Dodick, 2018). In line with our initial hypothesis, we observed a patient-specific pattern of the cortical intensity coding of CM, which is not reflected in the group statistics; this is echoed in the individual profiles of endogenous pain processing in each CBP patient (see a more in-depth discussion on individual patterns below). In other words, there are a number of regions that encode the pain intensity in CM; these regions are, however, specific for an individual and not commonly shared by all patients.

Our findings are not directly comparable with previous research on migraine as most imaging studies applied external (trigeminal) stimuli to elicit additional pain (Stankewitz et al., 2011; Stankewitz, Schulz, & May, 2013). Additionally, most of these studies investigated episodic migraine patients. In contrast, our study utilised patients

suffering from CM who were examined during attack-free phases. Patients were continuously evaluating different levels of their daily endogenous pain without any external nociceptive input. The few fMRI studies on CM suggest functional, structural, and neurochemical alterations of cortical and subcortical regions (Lerebours et al., 2019; Niddam et al., 2018; Planchuelo-Gómez et al., 2020; Schulte et al., 2017) and networks (Androulakis et al., 2017; Androulakis, Rorden, Peterlin, & Krebs, 2018; Coppola et al., 2019) compared to patients with episodic migraine or healthy controls. In line with these findings, our results may point to a neuronal reorganisation in CM patients which is specific for each individual.

4.1.1 | Analysing the temporal dynamics of a continuous design

For the present investigation, we kept and analysed the full dynamics of the fluctuating endogenous pain perception of patients with chronic pain; we did not define any statistical "events" such as periods of high pain or periods of increasing pain, but instead took the entire naturally evolving trajectory of pain into account. We also applied a very long time constant for high-pass filtering the data to preserve the natural shape of the pain-rating time course. This preservation also excluded any direct correction for autocorrelation, which could have otherwise destroyed the natural structure of the data (see Section 2 for a more suitable strategy regarding the correction of autocorrelation for continuous data). Furthermore, we did not include patients who would not exceed a certain amount of pain fluctuation, that is, by excluding recordings with insufficient fluctuations or even steadily increasing pain. The extended duration of the experiment guaranteed balanced phases of increasing, stable, and decreasing pain, which disentangled the processes related to pain intensity from aspects of pain intensity changes in all patients (see single session pain rating trajectories in Supplementary Figures 2 and 3).

4.2 | Encoding of the change of pain intensity across all patients—SLP

Although the fluctuating pain intensity represents an important daily life experience of patients with chronic pain, this phenomenon is barely investigated. Here, we explored how the processing of pain intensity changes is subserved in the brain and found that the change of endogenous pain of CBP patients is mainly encoded in the AIC and in frontal regions. Regions that show increased activity during falling pain were found in the occipital lobe (occipital pole, lateral occipital cortex), the PCC, pACC, and precuneus. For CM patients, positive relations were located in the AIC and the cerebellum. Besides occipital regions, negative relations were found in the precuneus and the angular gyrus.

Similar to our results, Baliki et al. reported increased activity in the right AIC and the cerebellum, but showed additional activity in the posterior insula, S2, multiple portions of the middle cingulate cortex,

and S1 (Baliki et al., 2006). However, these findings apply to periods of increasing pain contrasted to both periods of stable and decreasing pain. Therefore, the analysed periods of increasing pain are more influenced by pain-unspecific effects of motor activity and decision-making, which have a stronger effect on the BOLD amplitude. In the present study, we have controlled for these aspects of motor activity and decision-making by contrasting time periods of rising pain with periods of falling pain. Due to further prerequisites of balanced and fluctuating pain ratings, the analysis of pain changes can be considered as independent from the analysis of pain amplitude: increasing pain can occur at both high and low levels of pain. The regions that encode the change of pain experience could have an impact on the emotional well-being of the patients and would be a valuable target for therapeutic interventions such as neurofeedback.

4.3 | The role of the anterior insula for the processing of chronic pain

For both pain diseases, we found the largest cortical effect for pain direction encoding (SLP) in the AIC; rising endogenous pain is accompanied by increasing insular activity. Interestingly, for CBP the AIC is processing the intensity (AMP) and the change of pain intensity (SLP). However, the encoding of intensity exhibits a different temporal profile and has its peak after the processing change detection. Therefore, the activity of the AIC for amplitude and change of amplitude is overlapping and is determined by a summation of the activity for the current pain intensity and the transient activity for rising (plus) or falling (minus) pain. The results of the present investigation, in particular the contribution of the AIC, does not exclude that patients with chronic pain suffer from emotional problems (Baliki et al., 2006; Hashmi et al., 2013), but militates against opinions that the transitions to chronic pain might be reflected by a shift from insular processes to frontal areas. Our findings argue against suggestions that chronic pain may have become decoupled from cognitive insular processes but has turned into disease that is largely characterised by a negative emotional state in reference to the self. This is particularly true in light of the diversity of the single-subject findings.

4.4 | Individual patterns of pain intensity encoding in single patients

A major aspect of our investigation is the assessment of a single patient's profile of pain processing. In order to describe unique patterns of pain processing, each participant was recorded four times. As a result, the individual maps differ remarkably from each other and we found a substantial variation for the correlation of single patient signatures with the activity pattern from the group statistics. For CBP, the activity of the prominent regions of the group statistics may have been driven by the few patients who exhibit strong effects in the AIC and the pACC (see Supplementary Figures 4 and 7). As research articles usually do not publish single patient maps, we can only speculate

whether this phenomenon can be generalised. Indeed, the importance of assessing individual patterns of brain structure and activity has been suggested previously (Martucci, Ng, & Mackey, 2014).

Studies that address single patient effects have reported some variability (Gordon et al., 2017; Greene et al., 2019; Marek et al., 2018). In a similar vein, and although group statistics suggest otherwise, individual parameters of gamma oscillations in tonic and chronic pain show that pain is not encoded by gamma activity in all study participants (May et al., 2019; Schulz et al., 2015). The enormous variability of the individual pain signatures indicates qualitative rather than quantitative differences between patients (Zadelaar et al., 2019). If this phenomenon would be true, this would suggest that the currently discussed "replication crisis" (Huber, Potter, & Huszar, 2019; Open Science Collaboration, 2015) in neuroimaging would rather be a "sample crisis," for which the replication of an effect would depend on whether the repeated study had included a similar "dominant" subsample of participants showing similar activity patterns.

For these reasons, we initially decided against a direct comparison of the brain processes of CM and CBP patient groups. In our view, due to the large variability within each group, the results do not reflect a "true" difference between CBP and CM. The significant voxels are likely driven by a few CBP patients.

Indeed, the different pain signatures in the present study depict a complex picture: even if all patients had a marginal (and positively correlated) contribution of the insular cortex (which they do not have), we must assume that the major weight for the encoding of pain for most patients relies on the processing in different brain regions. The variety of cortical processing is in line with the clinical picture of pain diseases, in which each individual exhibits a complex composite of specific characteristics (Smith, 2009).

We cannot exclude that some variables such as disease duration, psychological parameters, current medication, the current average pain intensity, or indeed subgroups of the pain disease would modulate some aspects for a specific individual. However, the lack of significant and consistent positively correlated insular activity in most patients is suggested to be caused by qualitative rather than gradual differences between patients and would make the interpretation of quantitative effects challenging.

The question is, whether it is plausible that the encoding of pain in the insula (or any other region) can be modulated (e.g., by parameters like depression) in a way that some patients have a positive correlation between pain and brain activity and some patients would have negative relationships between brain activity and pain. The same applies for the pACC, which is considered to be a main hub of the descending pain control system. The group results suggest a negative relationship, but some individuals exhibit a positive relationship between the pACC and pain intensity, which would turn this region into a pain facilitation region rather than a pain inhibition hub. In other words, can some factors reverse the relationship between cortical activity and pain intensity? The plausibility of this potential phenomenon decides whether a correlation or modulation of any factor with the present variety of cortical maps is justified. In other words, an analysis that shows a modulation of cortical activity for data exclusively in the positive (or negative) range is indeed plausible and interpretable. In our view, a modulation that spans from negative to positive data requires a separate and thorough analysis of the function of this region. A mere correlation does not suffice. For the present study, we interpret the qualitatively different pattern as being modulated by other variables or subgroups as not plausible and therefore we deliberately rejected the idea of relating any behavioural variable to cortical data.

To consider individual *qualitative* variation as noise might indeed limit our understanding of pain processing. These "noisy" aspects may reflect how a patient is experiencing, encoding, and coping with pain, which can open a window for a better treatment of chronic pain. Therefore, assessing individual pain signatures could facilitate more accurate assessment of chronic pain conditions, which is in line with recent developments to enhance and promote individually tailored treatments in medicine (Mun et al., 2019; Ott et al., 2017).

Furthermore, our sample spans a broad range of disease years. However, the duration of the chronic pain disease does not appear to have a large impact on the topography of pain encoding as the single-subject encoding maps appear to be as diverse for patients with longer pain duration as for patients with shorter pain duration.

4.5 | Limitations

The present investigation included a large sample of patients with repeated recordings. Although the entire data amounts to more than 100 min of pain encoding data for each single patient, to regard individual variations of the data merely as noise may in fact hinder our understanding of sensory processing.

There are a few limitations that need to be considered. The majority of patients were on different types of prescribed medication which could have had an effect on the BOLD fluctuations. In addition, even the four recordings for each patient might not be enough to assess the stable and invariant pain signature of an individual. Similarly, the statistics on single patients might have been driven by a subset of the recordings. The investigation on the stability of the individual pattern of pain-related cortical activity across the four recordings, however, would require a different methodological approach, i.e. machine learning tools.

This undoubtedly mandatory analysis would overflow the amount of information that can be delivered in a single publication. The investigation of stability across sessions requires new statistical approaches and extensive methodological descriptions which will be addressed in a subsequent study.

In addition, we had to exclude a few participants with a rating time course that was not suitable for our investigation. Although these participants exhibited chronic pain, time courses with insufficient variability and/or slowly rising pain across the entire experiment are incompatible regarding experimental (effect of order, statistical independence of AMP and SLP) or technical (mandatory high-pass filtering) requirements.

Caution needs to be taken for the interpretation of the timing of the effects (see shifting section in Supplementary Material). Although we can determine the largest effect of the BOLD signal in reference to the current pain rating, the exact timing of the cascade of cortical processes that generate the current perception of pain is not possible. For example, the intensity of pain (AMP vector; Figure 2a, right) appears to be mainly encoded in the bilateral insula after slider movement. However, this simplified interpretation would ignore the fact that we (a) can observe a continuous increase of the BOLD response towards the peak and (b) face the unknown delay of the haemodynamic response in the insular cortex. Consequently, the slight difference of the haemodynamic response between left and right mid-insula cortex could be caused by actual differences in timing (faster left hemispheric processing) or by a slower haemodynamic response of the right mid-insular cortex compared to the left mid-insular cortex. For this reason, we can only interpret the statistical 3D maps but not the time courses of the haemodynamic response, which are included for illustration only.

5 | CONCLUSION

The present study expands the knowledge on the cortical underpinnings of chronic pain by showing that individuals exhibit their own signature of cortical processing of chronic pain; this applies to CBP as well as to CM. The individual cortical processing patterns are mostly not reflected by the results of the group statistics.

These key findings illustrate the limits of group statistics. The single subject maps cast some doubts on the usefulness and interpretability of the group findings and group comparisons on the encoding of pain: given the substantial qualitative variation of individual maps it is difficult to follow the conventional interpretation that the insular cortex encodes the experience of pain in CBP but not in CM. Furthermore, the current data suggest taking a closer look into the neuroimaging of other domains. Longitudinal studies could, one the one hand, identify the individually stable processes across several sessions, and on the other hand, follow the trajectory of individually unique changes in disease (e.g., the migraine cycle in Stankewitz et al., 2021) and healthy cortical processing (Greene et al., 2019; Sylvester et al., 2020). However, the approach on qualitative differences between subjects adds a substantial amount of complexity to the field but could explain some of the inconsistencies and failed replications in neuroscience. The current replication crisis may turn out to be a sample crisis, where findings could be replicated if follow-up studies have by chance included (dominating) participants with the same cortical effect as the previous study.

This finding is matched by the experience of clinicians; each patient can be characterised by a unique personality with various combinations of symptoms and a vast range of treatment success, which is reflected by a wide range of individual responses to medical treatment. In the quest to find the optimal treatment for each patient with chronic pain, the findings support recent developments for a more personalised medicine. Consequently, the present findings argue against a common biomarker for the subjective experience of chronic pain that is based on neuroimaging.

On the contrary, as the experimental setup was aimed to reflect the unique and natural trajectory of the subjective experience of pain, the data would support an individually tailored therapeutic approach in clinical settings. Further studies are needed to explore whether the current findings on individual pain signatures can be utilised for interventions that aim to directly modulate brain activity, for example, neurofeedback.

AUTHOR CONTRIBUTIONS

Astrid Mayr contributed to data acquisition, analysis of the data, drafting manuscript and figures. **Enrico Schulz** contributed to the conception and design of the study, acquisition and analysis of the data, and drafting manuscript and figures. **Pauline Jahn** and **Bettina Deak** contributed to the acquisition and analysis of the data. **Anne Stankewitz** contributed to the conception and design of the study and drafting the manuscript. **Ozan Eren** and **Andreas Straube** contributed to drafting the manuscript. **Viktor Witkovsky** and **Anderson Winkler** contributed to the analysis of the data and drafting the manuscript. All authors discussed the findings of the statistical analyses.

CONFLICT OF INTERESTS

The authors declare no potential conflict of interests.

DATA AVAILABILITY STATEMENT

The dataset is available at the Open Science Framework (https://osf.io/65c7n/).

ORCID

Enrico Schulz https://orcid.org/0000-0001-8188-380X

REFERENCES

Androulakis, X. M., Krebs, K., Peterlin, B. L., Zhang, T., Maleki, N., Sen, S., … Herath, P. (2017). Modulation of intrinsic resting-state fMRI networks in women with chronic migraine. *Neurology*, *89*, 163–169.

Androulakis, X. M., Rorden, C., Peterlin, B. L., & Krebs, K. (2018). Modulation of salience network intranetwork resting state functional connectivity in women with chronic migraine. *Cephalalgia*, *38*, 1731–1741.

Apkarian, A. V., Bushnell, M. C., Treede, R.-D., & Zubieta, J.-K. (2005). Human brain mechanisms of pain perception and regulation in health and disease. *European Journal of Pain*, *9*, 463–484.

Baliki, M. N., Baria, A. T., & Apkarian, A. V. (2011). The cortical rhythms of chronic back pain. *The Journal of Neuroscience*, *31*, 13981–13990.

Baliki, M. N., Chialvo, D. R., Geha, P. Y., Levy, R. M., Harden, R. N., Parrish, T. B., & Apkarian, A. V. (2006). Chronic pain and the emotional brain: Specific brain activity associated with spontaneous fluctuations

of intensity of chronic back pain. *The Journal of Neuroscience, 26,* 12165–12173.

Baliki, M. N., Geha, P. Y., Fields, H. L., & Apkarian, A. V. (2010). Predicting value of pain and analgesia: Nucleus accumbens response to noxious stimuli changes in the presence of chronic pain. *Neuron, 66,* 149–160.

Bezanson, J., Edelman, A., Karpinski, S., & Shah, V. B. (2015). Julia: A fresh approach to numerical computing. *SIAM Review, 59,* 65–98.

Burstein, R., Noseda, R., & Borsook, D. (2015). Migraine: Multiple processes, complex pathophysiology. *The Journal of Neuroscience, 35,* 6619–6629.

Callan, D., Mills, L., Nott, C., England, R., & England, S. (2014). A tool for classifying individuals with chronic Back pain: Using multivariate pattern analysis with functional magnetic resonance imaging data. *PLoS One, 9,* e98007.

Casser, H. R., Hüppe, M., Kohlmann, T., Korb, J., Lindena, G., Maier, C., ... Thoma, R. (2012). Deutscher Schmerzfragebogen (DSF) und standardisierte Dokumentation mit KEDOQ-Schmerz. *Der Schmerz, 26,* 168–175.

Coppola, G., Di Renzo, A., Petolicchio, B., Tinelli, E., Di Lorenzo, C., Parisi, V., ... Pierelli, F. (2019). Aberrant interactions of cortical networks in chronic migraine: A resting-state fMRI study. *Neurology, 92,* e2550–e2558.

Diers, M., Koeppe, C., Diesch, E., Stolle, A. M., Hölzl, R., Schiltenwolf, M., ... Flor, H. (2007). Central processing of acute muscle pain in chronic low back pain patients: An EEG mapping study. *Journal of Clinical Neurophysiology, 24,* 76–83.

Dodick, D. W. (2018). A phase-by-phase review of migraine pathophysiology. *Headache, 58,* 4–16.

Edwards, R. R. (2005). Individual differences in endogenous pain modulation as a risk factor for chronic pain. *Neurology, 65,* 437–443. https://doi.org/10.1212/01.wnl.0000171862.17301.84

Filippi, M., & Messina, R. (2020). The chronic migraine brain: What have we learned from neuroimaging? *Frontiers in Neurology, 10, 1356.* https://doi.org/10.3389/fneur.2019.01356/full

Giesecke, T., Gracely, R. H., Grant, M. A. B., Nachemson, A., Petzke, F., Williams, D. A., & Clauw, D. J. (2004). Evidence of augmented central pain processing in idiopathic chronic low back pain. *Arthritis and Rheumatism, 50,* 613–623.

Gold, M. S., & Gebhart, G. F. (2010). Nociceptor sensitization in pain pathogenesis. *Nature Medicine, 16,* 1248–1257. https://doi.org/10.1038/nm.2235

Gollub, R. L., Kirsch, I., Maleki, N., Wasan, A. D., Edwards, R. R., Tu, Y., ... Kong, J. (2018). A functional neuroimaging study of expectancy effects on pain response in patients with knee osteoarthritis. *The Journal of Pain, 19,* 515–527.

Gordon, E. M., Laumann, T. O., Gilmore, A. W., Newbold, D. J., Greene, D. J., Berg, J. J., ... Dosenbach, N. U. F. (2017). Precision functional mapping of individual human brains. *Neuron, 95,* 791–807.e7.

Gracely, R. H., Petzke, F., Wolf, J. M., & Clauw, D. J. (2002). Functional magnetic resonance imaging evidence of augmented pain processing in fibromyalgia. *Arthritis and Rheumatism, 46,* 1333–1343.

Greene, D. J., Marek, S., Gordon, E. M., Siegel, J. S., Gratton, C., Laumann, T. O., ... Dosenbach, N. U. F. (2019). Integrative and network-specific connectivity of the basal ganglia and thalamus defined in individuals. *Neuron, 105,* 742–758.e6. https://doi.org/10.1016/j.neuron.2019.11.012

Griffanti, L., Salimi-Khorshidi, G., Beckmann, C. F., Auerbach, E. J., Douaud, G., Sexton, C. E., ... Smith, S. M. (2014). ICA-based artefact removal and accelerated fMRI acquisition for improved resting state network imaging. *NeuroImage, 95,* 232–247.

Grossi, D. B., Chaves, T. C., Gonçalves, M. C., Moreira, V. C., Canonica, A. C., Florencio, L. L., ... Bigal, M. E. (2011). Pressure pain threshold in the craniocervical muscles of women with episodic and chronic migraine: A controlled study. *Arquivos de Neuro-Psiquiatria, 69,* 607–612.

Hashmi, J. A., Baliki, M. N., Huang, L., Baria, A. T., Torbey, S., Hermann, K. M., ... Apkarian, A. V. (2013). Shape shifting pain: Chronification of back pain shifts brain representation from nociceptive to emotional circuits. *Brain, 136,* 2751–2768.

Hashmi, J. A., Baliki, M. N., Huang, L., Parks, E. L., Chanda, M. L., Schnitzer, T., & Apkarian, A. V. (2012). Lidocaine patch (5%) is no more potent than placebo in treating chronic back pain when tested in a randomised double blind placebo controlled brain imaging study. *Molecular Pain, 8,* 29.

Hashmi, J. A., Baria, A. T., Baliki, M. N., Huang, L., Schnitzer, T. J., & Apkarian, A. V. (2012). Brain networks predicting placebo analgesia in a clinical trial for chronic back pain. *Pain, 153,* 2393–2402.

Headache Classification Committee of the International Headache Society (IHS). (2018). The international classification of headache disorders, 3rd edition. *Cephalalgia, 38,* 1–211.

Henderson, L. A., Peck, C. C., Petersen, E. T., Rae, C. D., Youssef, A. M., Reeves, J. M., ... Gustin, S. M. (2013). Chronic pain: Lost inhibition? *The Journal of Neuroscience, 33,* 7574–7582.

Huber, D. E., Potter, K. W., & Huszar, L. D. (2019). Less "story" and more "reliability" in cognitive neuroscience. *Cortex, 113,* 347–349.

Jenkinson, M., Beckmann, C. F., Behrens, T. E. J., Woolrich, M. W., & Smith, S. M. (2012). FSL. *NeuroImage, 62,* 782–790.

Kelly, R. E., Alexopoulos, G. S., Wang, Z., Gunning, F. M., Murphy, C. F., Morimoto, S. S., ... Hoptman, M. J. (2010). Visual inspection of independent components: Defining a procedure for artifact removal from fMRI data. *Journal of Neuroscience Methods, 189,* 233–245.

Kobayashi, Y., Kurata, J., Sekiguchi, M., Kokubun, M., Akaishizawa, T., Chiba, Y., ... Kikuchi, S.-I. (2009). Augmented cerebral activation by lumbar mechanical stimulus in chronic low back pain patients: An FMRI study. *Spine, 34,* 2431–2436.

Lerebours, F., Boulanouar, K., Barège, M., Denuelle, M., Bonneville, F., Payoux, P., ... Fabre, N. (2019). Functional connectivity of hypothalamus in chronic migraine with medication overuse. *Cephalalgia, 39,* 892–899.

Lloyd, D., Findlay, G., Roberts, N., & Nurmikko, T. (2008). Differences in low Back pain behavior are reflected in the cerebral response to tactile stimulation of the lower Back. *Spine, 33,* 1372–1377.

Lovibond, P. F., & Lovibond, S. H. (1995). The structure of negative emotional states: Comparison of the Depression Anxiety Stress Scales (DASS) with the Beck depression and anxiety inventories. *Behaviour Research and Therapy, 33,* 335–343. https://doi.org/10.1016/0005-7967(94)00075-u

Makary, M. M., Polosecki, P., Cecchi, G. A., DeAraujo, I. E., Barron, D. S., Constable, T. R., ... Geha, P. (2020). Loss of nucleus accumbens low-frequency fluctuations is a signature of chronic pain. *Proceedings of the National Academy of Sciences of the United States of America, 117,* 10015–10023.

Malinen, S., Vartiainen, N., Hlushchuk, Y., Koskinen, M., Ramkumar, P., Forss, N., ... Hari, R. (2010). Aberrant temporal and spatial brain activity during rest in patients with chronic pain. *Proceedings of the National Academy of Sciences of the United States of America, 107,* 6493–6497.

Marek, S., Siegel, J. S., Gordon, E. M., Raut, R. V., Gratton, C., Newbold, D. J., ... Dosenbach, N. U. F. (2018). Spatial and temporal organization of the individual human cerebellum. *Neuron, 100,* 977–993.e7.

Martucci, K. T., Ng, P., & Mackey, S. (2014). Neuroimaging chronic pain: What have we learned and where are we going? *Future Neurology, 9,* 615–626.

May, E. S., Nickel, M. M., Dinh, S. T., Tiemann, L., Heitmann, H., Voth, I., ... Ploner, M. (2019). Prefrontal gamma oscillations reflect ongoing pain intensity in chronic back pain patients. *Human Brain Mapping, 40,* 293–305.

Merskey, H., & Bogduk, N. (1994). *Classification of chronic pain, IASP task force on taxonomy.* Seattle, WA: International Association for the Study of Pain Press (Also available online at www.iasp-painorg).

Moriarty, O., McGuire, B. E., & Finn, D. P. (2011). The effect of pain on cognitive function: A review of clinical and preclinical research. *Progress in Neurobiology*, *93*, 385–404.

Mun, C. J., Suk, H. W., Davis, M. C., Karoly, P., Finan, P., Tennen, H., & Jensen, M. P. (2019). Investigating intraindividual pain variability: Methods, applications, issues, and directions. *Pain*, *160*, 2415–2429.

Niddam, D. M., Lai, K.-L., Tsai, S.-Y., Lin, Y.-R., Chen, W.-T., Fuh, J.-L., & Wang, S.-J. (2018). Neurochemical changes in the medial wall of the brain in chronic migraine. *Brain*, *141*, 377–390.

Open Science Collaboration. (2015). PSYCHOLOGY. Estimating the reproducibility of psychological science. *Science*, *349*, aac4716.

Ott, P. A., Hu, Z., Keskin, D. B., Shukla, S. A., Sun, J., Bozym, D. J., ... Wu, C. J. (2017). An immunogenic personal neoantigen vaccine for patients with melanoma. *Nature*, *547*, 217–221.

Penny, W. D., Friston, K. J., Ashburner, J. T., Kiebel, S. J., & Nichols, T. E. (2011). *Statistical parametric mapping: The analysis of functional brain images*. Amsterdam, Netherlands: Elsevier.

Phillips, C. J. (2009). The cost and burden of chronic pain. *Reviews in Pain*, *3*, 2–5.

Planchuelo-Gómez, Á., García-Azorín, D., Guerrero, Á. L., Aja-Fernández, S., Rodríguez, M., & de Luis-García, R. (2020). Structural connectivity alterations in chronic and episodic migraine: A diffusion magnetic resonance imaging connectomics study. *Cephalalgia*, *40*, 367–383.

Price, D. D. (2000). Psychological and neural mechanisms of the affective dimension of pain. *Science*, *288*, 1769–1772.

Salimi-Khorshidi, G., Douaud, G., Beckmann, C. F., Glasser, M. F., Griffanti, L., & Smith, S. M. (2014). Automatic denoising of functional MRI data: Combining independent component analysis and hierarchical fusion of classifiers. *NeuroImage*, *90*, 449–468.

Schreiber, T., & Schmitz, A. (1996). Improved surrogate data for nonlinearity tests. *Physical Review Letters*, *77*, 635–638.

Schulte, L. H., Allers, A., & May, A. (2017). Hypothalamus as a mediator of chronic migraine: Evidence from high-resolution fMRI. *Neurology*, *88*, 2011–2016.

Schulz, E., May, E. S., Postorino, M., Tiemann, L., Nickel, M. M., Witkovsky, V., ... Ploner, M. (2015). Prefrontal gamma oscillations encode tonic pain in humans. *Cerebral Cortex*, *25*, 4407–4414.

Schulz, E., Stankewitz, A., Witkovský, V., Winkler, A. M., & Tracey, I. (2019). Strategy-dependent modulation of cortical pain circuits for the attenuation of pain. *Cortex*, *113*, 255–266.

Schwedt, T. J., Krauss, M. J., Frey, K., & Gereau, R. W. (2011). Episodic and chronic migraineurs are hypersensitive to thermal stimuli between migraine attacks. *Cephalalgia*, *31*, 6–12.

Smith, H. S. (2009). *Current therapy in pain*. Amsterdam, Netherlands: Elsevier Health Sciences.

Stankewitz, A., Aderjan, D., Eippert, F., & May, A. (2011). Trigeminal nociceptive transmission in migraineurs predicts migraine attacks. *The Journal of Neuroscience*, *31*, 1937–1943.

Stankewitz, A., Keidel, L., Rehm, M., Irving, S., Kaczmarz, S., Preibisch, C., ... Toelle T. R. (2021). Migraine attacks as a result of hypothalamic loss of control. *NeuroImage: Clinical*, *32*, 102784.

Stankewitz, A., Schulz, E., & May, A. (2013). Neuronal correlates of impaired habituation in response to repeated trigemino-nociceptive but not to olfactory input in migraineurs: An fMRI study. *Cephalalgia*, *33*, 256–265.

Staud, R. (2012). Abnormal endogenous pain modulation is a shared characteristic of many chronic pain conditions. *Expert Review of Neurotherapeutics*, *12*, 577–585.

Sullivan, M. J. L., Bishop, S. R., & Pivik, J. (1995). The Pain Catastrophizing Scale: Development and validation. *Psychological Assessment*, *7*, 524–532.

Sylvester, C. M., Yu, Q., Srivastava, A. B., Marek, S., Zheng, A., Alexopoulos, D., ... Dosenbach, N. U. F. (2020). Individual-specific functional connectivity of the amygdala: A substrate for precision psychiatry. *Proceedings of the National Academy of Sciences of the United States of America*, *117*, 3808–3818.

Vachon-Presseau, E., Roy, M., Woo, C.-W., Kunz, M., Martel, M.-O., Sullivan, M. J., ... Rainville, P. (2016). Multiple faces of pain: Effects of chronic pain on the brain regulation of facial expression. *Pain*, *157*, 1819–1830.

Wager, T. D., Atlas, L. Y., Lindquist, M. A., Roy, M., Woo, C.-W., & Kross, E. (2013). An fMRI-based neurologic signature of physical pain. *The New England Journal of Medicine*, *368*, 1388–1397.

Winkler, A. M., Ridgway, G. R., Webster, M. A., Smith, S. M., & Nichols, T. E. (2014). Permutation inference for the general linear model. *NeuroImage*, *92*, 381–397.

Winkler, A. M., Webster, M. A., Brooks, J. C., Tracey, I., Smith, S. M., & Nichols, T. E. (2016). Non-parametric combination and related permutation tests for neuroimaging. *Human Brain Mapping*, *37*, 1486–1511.

Zadelaar, J. N., Weeda, W. D., Waldorp, L. J., Van Duijvenvoorde, A. C. K., Blankenstein, N. E., & Huizenga, H. M. (2019). Are individual differences quantitative or qualitative? An integrated behavioral and fMRI MIMIC approach. *NeuroImage*, *202*, 116058.

SUPPORTING INFORMATION

Additional supporting information may be found in the online version of the article at the publisher's website.